Early Diagnosis of Alzheimer's Disease Using Deep Learning

Huanhuan Ji
Guilin University of Electronic Technology
Guilin, China

Zhenbing Liu
Guilin University of Electronic Technology
Guilin, China

Wei Qi Yan
Auckland University of Technology
Auckland, New Zealand

Reinhard Klette
Auckland University of Technology
Auckland, New Zealand

ABSTRACT

Alzheimer's disease (AD) leads to memory loss and impairment, which may cause further symptoms. It affects lives of patients seriously and is not curable, but early confirmation of AD may be helpful to start proper treatment so as to avoid further brain damage. Over the past decades, machine learning methods have been applied to the classification of AD with results based on manually prepared features and a classifier having a multiple-step architecture. Recently, with the development of deep learning, the end-to-end process of neural networks has been employed for pattern classification. In this paper, we focus on early diagnosis of AD based on convolutional neural networks (ConvNets) by using magnetic resonance imaging (MRI). Image slices of gray matter and white matter from MRI have been used as the inputs for classification. Ensemble learning methods have been employed after the convolutional operations for improving the classification by combining outputs of deep learning classifiers [27]. Three base ConvNets were designed, implemented, and compared in this paper. Our method was evaluated based on a dataset from the Alzheimer's Disease Neuroimaging Initiative for the early diagnosis of this illness. In particular, the accuracy rates of our classifications have reached up to 97.65% for AD/mild cognitive impairment and 88.37% for mild cognitive impairment/normal control.

CCS CONCEPTS

• **Computing methodologies** → *Object recognition*; *Neural networks*; • **Applied computing** → *Health informatics*.

KEYWORDS

Alzheimer's disease, ConvNets, ensemble learning, magnetic resonance imaging

1 INTRODUCTION

Alzheimer's disease (AD) is a neurodegenerative sickness which usually occurs in older people and easily destroys human memorization and behaviors. It was reported that there are 26.6 million AD cases worldwide, including 14.99 million cases that are at an early stage in 2006. It is predicted to affect one out of 85 people globally. The number of AD populations is estimated to increase to 106.8 million by 2050 [2].

AD can be divided into three phases: *Normal control* (NC), *mild cognitive impairment* (MCI), and AD. The structure of the human brain shows little differences during the three phases. MCI, a prodromal stage of AD, is an important phase for clinical trials. It is possible to delay AD deterioration if it can be detected during the prodromal stage. In MCI, individuals have a mild change on behaviors that can be observed easily by any people who are close to the patients. *Magnetic resonance imaging* (MRI) was employed to visualize the images from these three phases. MRI can provide a clear 3D structure while being noninvasive for the diagnosis. As we know, MRI has been successfully applied to the computer-aided diagnosis by segmenting the images of *gray matter* (GM) and *white matter* (WM) to classify the AD and NC [4][5][17]. In this paper, GM and WM are preprocessed and classified based on our proposed deep learning model.

Multiple methods have been exploited to aid the diagnosis of AD [14]. Over the past decades, machine learning methods have been employed for the classification of AD with a good performance. The general process of machine learning aided diagnosis using MRI can be grouped into three fundamental phases [18]: (1) Predetermination of regions-of-interest (ROIs), (2) extraction/ selection of features from ROIs, and (3) construction of classification models for features. But the features were generated and extracted manually from the MRI data. Because of the problem of high dimensionality of features and small number of samples on medical images, various methods [3][10][24] for solving this problem have been proposed.

Zhu et al. [29] embedded relational information inherently into a sparse multi-task learning framework so as to select the features. Ortiz et al. [15] proposed to use the mean of *learning vector quantization* (LVQ) to model the tissue distribution; then, SVM was adopted as the classifier. Other work has been employed to train a classifier with a sub-optimal performance, due to the heterogeneous nature between feature extraction and classifier.

Deep learning is a revolutionizing methodology compared to traditional machine learning methods. Instead of separating feature extraction from a classifier, deep learning can learn the parameters of neural networks directly from the images without an engagement of human experts. Recently, convolutional neural networks have achieved very high average precision on pattern classifications using digital images [12]; especially it has shown the successful applications on computer-aided diagnosis (CAD) [21][23][28].

ICCCV'19, June 15–18, 2019, Jeju Island, South Korea

ACM ISBN 978-1-4503-6322-8/19/06…$15.00
https://doi.org/10.1145/3341016.3341024

Gupta et al. used *sparse autoencoder* (SAE) to learn a set of natural images and then applied convolutional network for AD classification [6]. Sarraf et al. used the convolutional neural networks and the LeNet-5 to classify Alzheimer's disease from normal controls with the accuracy 96.85% [20]. Shi et al. [22] proposed multimodal stacked deep polynomial networks to fuse multimodal neuroimaging data for AD diagnosis.

Ciprian et al. [1] modified the 16 layers VGGNet for the three ways classification of AD, MCI, and NC based on the *Alzheimer's disease neuroimaging initiative* (ADNI) dataset and achieved an overall accuracy 91.85%. Liu, et al. [11] proposed a zero-masking scheme for data fusion so as to extract complementary information from multiple data modalities. Lian et al. [9] proposed a *hierarchical fully convolutional network* (H-FCN) to automatically identify local patches and regions in the whole brain MRI for AD diagnosis. Suk et al. [25] proposed to combine two methods based on sparse regression and deep learning for AD diagnosis.

Islam et al. [8] improved a CNN model based on the Inception-V4 neural network [26] with the *open-access series of imaging studies* (OASIS) database [13]. Andres et al. [16] used *deep belief networks* (DBN) as the base classifiers, the final prediction was determined by using a voting scheme.

Transfer learning has been adopted for the CAD using deep *convolutional neural networks* (CNNs or ConvNets) based on two databases [23]. For the small sample problem of medical images, transfer learning was used on the classification of AD. For ensemble learning, Islam, et al. proposed a new deep convolution neural networks for AD images detection and classification. DenseNet 121, 161, and 169 were used as the base classifiers, then the results were ensembled by using the well-trained weights.

Different to existing work, in this paper, we propose an ensemble classifier based on ConvNets. ResNet50 [7], NASNet [30], and MobileNet [19] as learners are combined together for the early diagnosis of AD. Our work mainly has the twofold contributions: (1) the base classifiers are trained by using the end-to-end process instead of directly extracting convolutional features for training classifiers, and (2) our ensemble learning is implemented using base learners to improve the performance of the early diagnosis of AD. The rest of this paper is organized as follows. In Section 2, we introduce our methods and the used database. In Section 3, our experimental results are described. Finally, conclusions are drawn at the end of this paper.

2 OUR METHODS

2.1 Database

In this paper, the data were grabbed from the ADNI database at adni.loni.usc.edu. ADNI especially was designed to collect, validate, and utilize the data such as MRI, *positron emission tomography* (PET) images and blood biomarkers as predictors for AD. ADNI was initiated in 2003 to collect and analyze AD, MCI, and NC brain images. A total of 615 MRI images were split into 179 AD, 254 MCI, and 182 NC in NifTI format. The ratio between male and female samples in each category is roughly equal. The data is usually categorized for training, validation, and test in a proportion of 3:1:1.

2.2 Preprocessing

MRI images from the ADNI database were corrected to exclude the influences on head movement because of long-time image acquisitions by using *statistical parametric mapping* (SPM), that is a software developed by the University of London based on the MATLAB platform. The images downloaded from the website were resized into $192 \times 192 \times 160$.

Then, the resized MRI images were grouped into WM, GM, and cerebrospinal fluid (CSF) categories by using SPM. The GM and WM images were selected as the dataset for training because the GM and WM can provide a clear and important brain structure for the diagnosis of AD.

After the segmentation, the GM and WM has been sliced into 192 images in TIF format. According to the prior knowledge, consecutive 20 slices with significant brain structure from each MRI image were selected as the data from GM and WM. The slices from GM were added to the collection from WM and resized into 224×224 as the inputs of our neural networks.

2.3 Network Architecture

Albeit conventional machine learning approaches took use of the features extracted by experts, we utilize deep learning with the end-to-end process to classify the AD. In this project, our model for early diagnosis of AD would be presented. The main framework of this paper is shown in Fig. 1.

In this project, there are three base classifiers which are employed for our experiments. Firstly, the data downloaded from ADNI are preprocessed, 20 slices with significant brain structures are selected and sent to the ConvNet for model training. Then, each base classifier exports a result of the slice. We integrate the 20 slices together in order to classify this subject. At last, the ensemble learning methods are employed on the output of each ConvNet network.

Unlike image datasets used in computer vision, the ImageNet offers a very comprehensive database with a lot of natural images which were used to train a deep learning model with huge parameters. It is difficult to train such a big model fully using a small medical database. Therefore, transfer learning was used on our experiment to improve the accuracy.

The previously trained network based on the ImageNet was used for our base classifier. As we know, the ConvNet for image classification is comprised of two parts: a series of pooling and convolutional layers as well as fully connected layers. In this paper, the first part of the ConvNet is convolution base (conv_base) consisting of a series of pooling and convolutional operations. Our fully connected layers with initialized weights were added to the base layer so as to combine the convolution base together. The structure of this classifier is shown as Fig 2.

Our entire base classifier consists of three parts. The first part and the second part form the convolution base. The third part is committed as fully connected layers. The training of each base classifier includes two stages. Firstly, the convolution base is fixed as we train the fully connected classifier in order to fit the weights of the fully connected layers. The fully connected layers are randomly

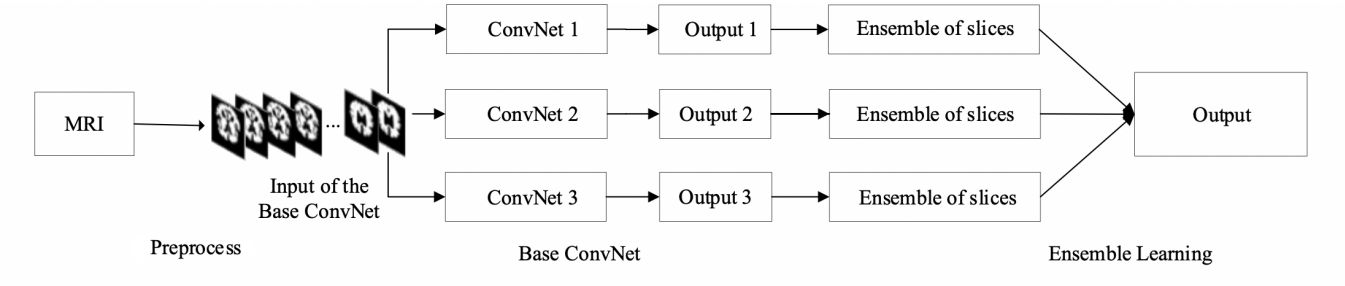

Figure 1: The overall framework is split into three parts: Preprocessing, ConvNets, and ensemble learning.

initialized, a large weight updates would be propagated. Otherwise, the network is modified that was previously learned by the ConvNet.

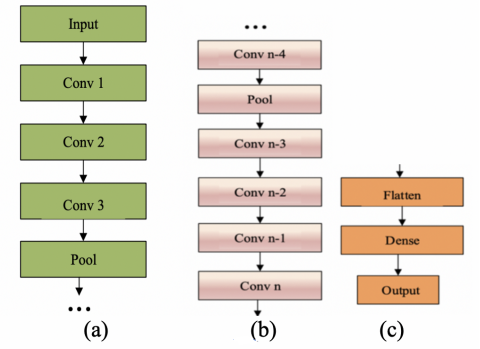

Figure 2: The structure of the base classifier ConvNet.

After the first phase, we release a few of top layers of the convolution based. Then, the base classifier is trained based on fine tuning to fit the early diagnosis of AD by using the end-to-end process. The first part of the convolution base has been fixed all the time. These base classifiers are eResNet50, eNASNet, and eMobileNet in this paper.

In the third part of this network, the outputs are flattened into a new layer. Then fully connected layers are added to the flatten layer. In order to avoid overfitting, a dropout layer was added to the fully connected layer. As we know, *backpropagation* (BP) of neural networks adjusts the weights and offsets of the hidden layers so as to match the output and the input.

Compared with BP neural networks, Bernoulli function is added to the network so as to adjust the weights and offsets of the hidden layers, avoid overfitting, and better match the inputs and outputs. The structure of our neural network with dropout is shown in Fig. 3. The workflow is expressed as follow:

$$\begin{aligned} r_j^{(l)} &\sim B(p) \\ \tilde{x}^{(l)} &= r^{(l)} x^{(l)} \\ y_i^{(l+1)} &= w_i^{(l+1)} \tilde{x}_i^{(l)} + b_i^{(l+1)} \\ x_i^{(l+1)} &= f(y_i^{(l+1)}) \end{aligned} \tag{1}$$

where $B(\cdot)$ is a Bernoulli (binomial) distribution, x denotes neurons in the layer l that is transferred to the next layer; $y_i^{(l+1)}$ is the output of the neurons of layer l on the $y_i, i = 1, \cdots, N$.

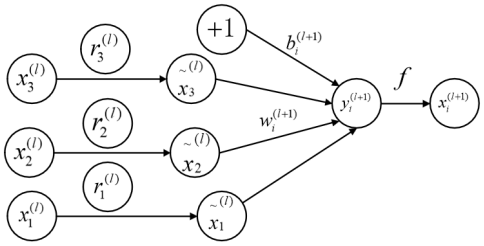

Figure 3: The dropout network.

3 EXPERIMENTS AND RESULTS

In this section, we validate our method mainly based on the comparisons: AD *vs* MCI and MCI *vs* NC. Firstly, bResNet50, bNASNet, and bMobileNet are used as the base learns for ensemble learning considered as the comparative experiment. Then, our method eResNet50, eNASNet, and eMobileNet are trained by using the end-to-end process for ensemble learning. Finally, our results are compared with the prevalent results on the classification of AD.

The proposed networks were implemented by using Python 3.5 with the Keras, and the computer we experimented facilities with a single GPU (i.e., NVIDIA DGX-1). During the preprocessing, SPM based on the MATLAB was used to deal with the data downloaded from ADNI. The Adam optimizer was used for training, the learning rate was set as 2.0×10^{-5} at the beginning, and the size of minibatch was initialized as 20.

Our method was mainly validated for early diagnosis of AD (i.e., AD *vs*. MCI, and MCI *vs*. NC). The classification was evaluated by using four measures: Classification accuracy (*ACC*), specificity (*SPE*), sensitivity (*SEN*), and the area under receiver operating

Table 1: Accuracy, sensitivity, specificity, and AUC of various classification methods for AD and MCI.

Models	ACC (%)	SEN (%)	SPE (%)	AUC
bResNet50	97.65	100.00	94.29	0.95
eResNet50	98.80	98.00	100.00	1.00
bNASNet	97.65	98.00	94.29	0.95
eNASNet	98.82	96.00	100.00	1.00
bMobileNet	97.64	98.00	94.28	0.95
eMobileNet	97.65	96.00	100.00	1.00
bEnsemble	98.82	98.00	100.00	0.95
eEnsemble	97.65	96.00	100.00	1.00

characteristic curve (*AUC*). These measures are recalled as follows:

$$ACC = \frac{TP + TN}{TP + TN + FP + FN} \quad (2)$$

$$SEN = \frac{TP}{TP + TN} \quad (3)$$

$$SPE = \frac{TN}{TN + FP} \quad (4)$$

where TP, TN, FP, and FN are the rates of true positive, true negative, false positive, and false negative. The AUC is calculated based on all possible pairs of SEN and SPE obtained by changing the thresholds of the classification scores yielded by using the trained networks.

4 COMPARISONS

In this paper, eResNet50, eNASNet, and eMobileNet were selected as the base classifiers which were trained by using the end-to-end process. The training of each base classifier includes two phases. Pertaining to eResNet50, the ConvNet is fixed as we train the fully connected classifier in order to fit the weights of the fully connected layers classifier. The fully connected layers on the top were randomly initialized, a large weight updates would be propagated. Then, a few top layers of convolution base were released and combined with the updated fully connected layers so as to fit the model for medical images. The base classifiers were trained based on fine tuning between fully connected layers and released layers of the network for the early diagnosis of AD by using the end-to-end process. The same operations were used based on eNASNet and eMobileNet to train the base learners.

As a comparison, a previously well-trained network was used for our experiments based on transfer learning, the classifier is trained by using ResNet50, NASNet, and MobileNet. The new networks are bResNet50, bNASNet, and bMobileNet. The results are used to compare with the data from our existing base classifiers: eResNet50, eNASNet, and eMobileNet. We test our model after training and ensemble the results of the base ConvNet on the classification of AD. The classification results for AD and MCI are shown as Table 1.

From Table 1, we see that all accuracy sensitivity and AUC values obtained from the models by using the end-to-end process are higher than those from the models trained by the base classifiers. Especially, the accuracy of eNASNet is 1.17% higher than that of bNASNet. The "bEnsemble" is the result after combining bResNet50, bNASNet, and bMobileNet. The "eEnsemble" is the result after ensembling eResNet50, eNASNet and eMobileNet. From "bEnsemble", we see that not only the accuracy of the ensemble is higher than that of the single model, but also the specificity is superior to the single model which shows the better performance of ensemble learning. The results between MCI and NC are shown in Table 2.

Table 2: Accuracy, sensitivity, specificity, and AUC of various classification methods for MCI and NC.

Models	ACC(%)	SEN(%)	SPE(%)	AUC
bResNet50	81.39	80.56	82.00	0.91
eResNet50	86.05	83.33	88.00	0.95
bNASNet	81.39	55.56	100.00	0.92
eNASNet	87.21	75.00	96.00	0.95
bMobileNet	81.39	55.56	100.00	0.92
eMobileNet	89.53	83.33	94.00	0.95
bEnsemble	80.23	58.33	96.00	0.91
eEnsemble	88.37	80.56	94.00	0.96

From Table 2, we see that the models trained by using the end-to-end method have better results than the models trained by using the features extracted from the base classifiers. Especially, the accuracy of "eEnsemble" has been improved 8.14% compared to the results of "bEnsemble"and the sensitivity of eNASNet is 0.19 higher than bNASNet. In the end, the AUC of "eEnsemble" is the highest one which demonstrates the effectiveness of our method. The receiver operating characteristic (ROC) curves for the comparisons between MCI and NC are shown in Fig. 4.

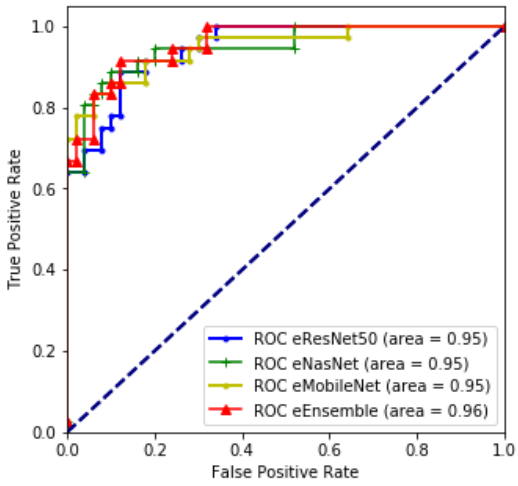

Figure 4: The ROC curves for the classification between MCI and NC using our own methods.

In this section, we compare our results with the previous work regarding to the diagnosis of AD. Table 3 shows the results of previous studies and our results. From Table 3, we see that our results have a better performance on the classifications of MCI. Our model has a higher accuracy of classification for AD and MCI.

Table 3: Comparisons of the results of previous studies and our method (%)

	AD *vs* NC			AD *vs* MCI			MCI *vs* NC		
References	ACC	SEN	SPE	ACC	SEN	SPE	ACC	SEN	SPE
Billones et al. [1]	98.33	98.89	97.78	90.00	91.67	97.78	91.67	92.22	91.11
Sarraf et al. [20]	98.84	-	-	-	-	-	-	-	-
Ortiz et al. [16]	90.09	86.12	94.10	84.00	79.12	89.12	83.14	67.26	95.09
Lian et al. [9]	90.30	82.40	96.50	-	-	-	-	-	-
Suk et al. [25]	91.02	92.72	89.94	-	-	-	73.02	77.60	68.22
Our method	98.59	97.22	**100.00**	**97.65**	**96.00**	**100.00**	88.37	80.56	94.00

5 CONCLUSION

In this paper, we proposed an ensemble learning method for the early diagnosis of AD by using deep learning. Specifically, we trained our base classifiers by using the end-to-end process. Firstly, we fixed the base learner and fit the fully connected layers. Then, we released a few layers on the top of the network combined with the updated fully connected layers so as to fit the model for learning abstract features of medical images. We trained the base classifier in order to fit the model better. In the end, the outputs of those base learners were ensembled to improve the accuracy and stability. The results based on the ADNI database show that our method is superior to the conventional machine learning approaches.

6 ACKNOWLEDGMENTS

This work was completed when the first author was a visiting scholar at the Auckland University of Technology, New Zealand. This project is supported by the study abroad program for graduate students of the Guilin University of Electronic Technology China. The data used in this paper was downloaded from the *Alzheimer's disease neuroimaging initiative* (ADNI) (see adni.loni.usc.edu). We like to acknowledge everyone who provided their support for this research project.

7 REFERENCES

[1] D. Billones, D. Demetria, and D. Hostallero. 2016. DemNet: A Convolutional Neural Network for the detection of Alzheimer's Disease and Mild Cognitive Impairment. In *TENCON*. IEEE, Singapore, 3724–3727.

[2] R. Brookmeyer, E. Johnson, and K. Zieglergraham. 2007. Forecasting the global burden of Alzheimer's disease. *Journal of the Alzheimers Association* 3, 3 (2007), 186–191.

[3] B. Cheng, D. Zhang, S. Chen, and D. Shen. 2011. Predicting Clinical Scores Using Semi-supervised Multimodal Relevance Vector Regression. In *Machine Learning in Medical Imaging(MLMI)*. Springer, Canada, 241–248.

[4] D. Chyzhykand, M. Grana, A. Savio, and J. Maiora. 2012. Hybrid dendritic computing with kernel-LICA applied to Alzheimer's disease detection in MRI. *Neurocomputing* 75, 1 (2012), 72–77.

[5] R. Cuingnet, E. Gerardin, and J. Tessieras. 2011. Automatic classification of patients with Alzheimer's disease from structural MRI: a comparison of ten methods using the ADNI database. *Neuroimage* 56, 2 (2011), 766–781.

[6] A. Gupta, M. Se, C. Ayhan, and A. Maida. 2013. Natural image bases to represent neuroimaging data. In *ICML'13*. JMLR, Atlanta, USA, 987–994.

[7] K. He, X. Zhang, and S. Ren. 2016. Deep Residual Learning for Image Recognition. In *CVPR*. IEEE, USA, 770–778.

[8] J. Islam and Y. Zhang. 2017. A Novel Deep Learning Based Multi-class Classification Method for Alzheimer's Disease Detection Using Brain MRI Data. In *Brain Informatics: International Conference*. Springer, China, 213 – 222.

[9] C. Lian, M. Liu, J. Zhang, and D. Shen. 2018. Hierarchical Fully Convolutional Network for Joint Atrophy Localization and Alzheimer's Disease Diagnosis using Structural MRI. *IEEE Transactions on PAMI* 2019, 12 (2018), 1–14.

[10] F. Liu, C. Wee, H. Chen, and D. Shen. 2014. Inter-modality relationship constrained multi-modality multi-task feature selection for Alzheimer's Disease and mild cognitive impairment identification. *NeuroImage* 84 (2014), 466–475.

[11] S. Liu and W. Cai. 2015. Multimodal neuroimaging feature learning for multiclass diagnosis of Alzheimer's disease. *IEEE Transactions on Biomedical Engineering* 62, 4 (2015), 1132 – 1140.

[12] Z. Liu, W. Yan, and B. Yang. 2018. Image denoising based on a CNN model. In *ICCAR*. IEEE, New Zealand, 389–393.

[13] D. Marcus, T. Wang, and J. Parker. 2007. Open access series of imaging studies (OASIS): Cross-sectional MRI data in young, middle aged, nondemented, and demented older adults. *Journal of Cognitive Neuroscience* 19, 9 (2007), 1498–1507.

[14] M. Nguyen, H. Le, W. Yan, and A. Dawda. 2017. A vision aid for the visually impaired using commodity dual-rear-camera smartphones. In *NIPS*. IEEE, New Zealand, 389–393.

[15] A. Ortiz, J. Gorriz, and J. Ramirez. 2013. LVQ-SVM Based CAD tool applied to structural MRI for the diagnosis of the Alzheimer's disease. *Pattern Recognition Letters* 34, 14 (2013), 1725–1733.

[16] A. Ortiz, J. Munilla, and M. Gorriz. 2016. Ensembles of Deep Learning Architectures for the Early Diagnosis of the Alzheimer's Disease. *International Journal of Neural Systems* 26, 7 (2016), 1132–1140.

[17] A. OrtizEmail, M. Jorge, and Francisco J. 2017. Learning Longitudinal MRI Patterns by SICE and Deep Learning: Assessing the Alzheimer's Disease Progression. In *Medical Image Understanding and Analysis*. Springer, United Kingdom, 413 – 424.

[18] S. Rathore, M. Habes, and M. Iftikhar. 2017. A review on neuroimaging-based classification studies and associated feature extraction methods for Alzheimer's disease and its prodromal stages. *NeuroImage* 155 (2017), 530–548.

[19] M. Sandler, G. Andrew, M. Zhu, A. Zhmoginov, and L. Chen. 2018. MobileNetV2: Inverted Residuals and Linear Bottlenecks. In *CVPR*. IEEE, USA, 4510–4520.

[20] S. Sarraf and G. Tofighi. 2016. Deep learning-based pipeline to recognize Alzheimer's disease using fMRI data. In *Future Technologies Conference*. IEEE, San Francisco, USA, 816 – 820.

[21] D. Shen, G. Wu, and H. Suk. 2017. Deep Learning in Medical Image Analysis. *Annual Review of Biomedical Engineering* 19, 1 (2017), 221–248.

[22] J. Shi, X. Zheng, and Y. Li. 2017. Multimodal Neuroimaging Feature Learning with Multimodal Stacked Deep Polynomial Networks for Diagnosis of Alzheimer's Disease. *IEEE Journal of Biomedical and Health Informatics* 22, 1 (2017), 173–183.

[23] H. Shin, H. Roth, and M. Gao. 2016. Deep Convolutional Neural Networks for Computer-Aided Detection: CNN Architectures, Dataset Characteristics and Transfer Learning. *IEEE Transactions on Medical Imaging* 35, 5 (2016), 1285–1298.

[24] H. Suk, S. Lee, and D. Shen. 2015. Deep sparse multi-task learning for feature selection in Alzheimer's disease diagnosis. *Brain Structure & Function* 221, 15 (2015), 2569–2587.

[25] H. Suk, W. Lee, and D. Shen. 2017. Deep ensemble learning of sparse regression models for brain disease diagnosis. *Medical Image Analysis* 37 (2017), 101–113.

[26] C. Szegedy, S. Ioffe, and V. Vanhoucke. 2017. Inception-v4, Inception-ResNet and the Impact of Residual Connections on Learning. In *Proceedings of AAAI'17*. AAAI, USA, 4278–4284.

[27] X. Wang and W. Yan. 2019. Multi-perspective gait recognition based on ensemble learning. *Springer Neural Computing and Applications* 31 (2019), 1–12.

[28] J. Zhang and Y. Gao. 2016. Detecting Anatomical Landmarks for Fast Alzheimer's Disease Diagnosis. *IEEE Transactions on Medical Imaging* 35, 12 (2016), 2524–2533.

[29] X. Zhu, H. Suk, and L. Wang. 2017. A novel relational regularization feature selection method for joint regression and classification in AD diagnosis. *Medical Image Analysis* 38 (2017), 205–214.

[30] B. Zoph, V. Vasudevan, J. Shlens, and Q. Le. 2018. Learning Transferable Architectures for Scalable Image Recognition. In *CVPR*. IEEE, USA, 8697–8710.